FEMLAB MODELING OF ELECTRIC FIELD AND INDUCED ELECTRIC FORCE ACTING ON CARBON NANOTUBE TIP IN DC PLASMA SHEATH

J.Blažek, P.Špatenka

University of South Bohemia, Group of Plasma Physics and Chemistry, Branišovská 31, CZ-370 05 České Budějovice, Czech Republic

Abstract

We have developed a code for MATLAB and FEMLAB programs for computation of electrical field and ion bombardment in the plasma sheath close to a negative biased electrode. Application of the program is demonstrated on calculations of the electric field in the vicinity of carbon nanotubes (CNTs) and the electric forces acting on their tips. The mechanism of CNTs oriented growth is not fully understood yet but our FEMLAB computations support the hypothesis that the CNTs alignment is caused by the electric forces acting on CNTs tips in the DC plasma sheath. To verify the reliability of the 3-D FEMLAB modeling we computed electric characteristics of a conductive sphere placed in a homogeneous electric field and compared them with their theoretical values.

Keywords: FEMLAB, electric force, plasma sheath, carbon nanotubes

Introduction

Carbon nanotubes (CNTs) have attracted much research effort since their discovery in 1991 [1]. Their unique structural, chemical, electrical and mechanical properties promise them to be an appropriate material for variety of applications, such as field emission sources, nanoelectronics devices or mechanical reinforcement in composite materials [2,3].

Depending on experimental conditions CNTs could grow in one direction (alignment) or in a curly fashion. Only a few attempts have been done to explain the mechanism of the oriented growth, but it is obvious that in a DC plasma sheath the electric field is responsible for the alignment. Yu et al. [4] supposed that the charged particles form bonds along the field lines. Chen et al. [5] expressed a hypothesis that the nanotubes are pulled in the direction of the electric field. Bower et al. [6] tried to estimate the electric field from the length of nanotubes and from the self-bias in the microwave discharge. They assessed the magnitude of the electric intensity to be $1 \cdot 10^5$ V/m.

In spite of the hypothesis the CNTs alignment is caused by the electric forces, so far nobody has computed their magnitude. Hence we have developed a code for MATLAB and FEMLAB programs in which both the electric field in the vicinity of CNTs tips and the electric forces acting on them are computed from experimentally measured bulk plasma parameters.

Basic equations

Almost the whole potential bias in the DC plasma is concentrated in a thin layer at the cathode – the sheath [7]. Due to the high negative voltage of the cathode the only ion number density n_i in the sheath can be taken into account. The electric field then satisfies the Poisson equation in the form

$$\nabla^2 U = -\frac{en_i}{\varepsilon_0} \quad \left(\vec{E} = -\nabla U\right) \tag{1}$$

Supposing negligible ionization in the sheath, the continuity equation

$$\nabla \cdot (n_i \vec{v}_i) \approx 0 \tag{2}$$

holds. The equation system is completed by an equation connecting the ion velocity $\vec{v}_i$ with the electric field. Assuming typical working pressure 10 mbar, the collisional ion drift motion has to be considered. Then [7]

$$\vec{v}_i = \mu_i \vec{E}, \quad \mu_i \equiv \frac{2}{\pi} \cdot \frac{e\lambda_i}{M_i |\vec{v}_i|} \tag{3}$$

where M_i and λ_i are the ion mass and ion mean free path, respectively.

Owing to the supposed conductive connection between the CNTs and the cathode the potential of the nanotubes is equal to the potential of the cathode. The normal component of the electric intensity in the symmetry plane between the neighboring nanotubes is zero. The boundary conditions specifying the outer boundary of the sheath are much more complicated and will not be discussed here.

3D equations (1) – (3) with corresponding boundary conditions represent five scalar equations for five scalar unknowns U, n_i, $\vec{v}_i$. As this system is ill – conditioned, it is impossible to solve it in FEMLAB directly. Fortunately, it could be shown that the electric field is distorted only in the close vicinage of CNTs tips and also the ion current is influenced by the CNTs presence negligibly. We exploited this fact as follows. First, we reduced the 3D system (1) – (3) with its boundary conditions to the 1D (planar) case without CNTs and solved this system analytically [7]. Second, we solved only the 3D Poisson equation in the vicinity of CNTs, with the ion density taken from the planar case. The 3D boundary conditions at the outer sheath edge were replaced by the undisturbed planar values at a level of several (e.g. 10) radii above the CNTs tips.

From the electric intensity one can easily determine the induced surface charge and electric force acting on the nanotube,

$$\sigma = \varepsilon_0 E \tag{4}$$

$$F = \frac{\varepsilon_0}{2} \int_S E^2 \cos\theta \, \mathrm{d}S \tag{5}$$

In these equations E is the intensity just above the nanotube surface S and θ is the angle between the normal to the nanotube surface and nanotube longitudinal axis.

Test of numerical reliability

Before solving the Poisson equation (1) for the CNTs by the 3D electrostatics application mode of FEMLAB the reliability of the implemented finite element method was tested on a problem with similar geometry and exactly known solution: The z - component of the electric field

$\vec{E} = (E_x, E_y, E_z)$ of a conductive sphere of a radius R placed in the originally homogeneous electric field $\vec{E}_0 = (0,0,E_0)$ is given by the relation

$$\gamma \equiv \frac{E_z}{E_0} = 1 + \left(\frac{R}{r}\right)^3 \cdot \left[3\left(\frac{z}{r}\right)^2 - 1\right] \tag{6}$$

The induced surface charge and electric force acting on the upper hemisphere are exactly

$$\sigma = 3\varepsilon_0 E_0 \cos\theta \tag{7}$$

$$F = \frac{9}{4}\pi\varepsilon_0 \cdot (RE_0)^2 \tag{8}$$

The FEMLAB command-line function solving this problem for $R = 1$, $E_0 = 1$ is listed in the Appendix. Figures 1,2 depict the computed field enhancement factor $\gamma \equiv E_z / E_0$ and its error. As is seen from these figures, the maximum error is reached just on the surface and therefore maximally influences the calculation of the force acting on the upper hemisphere. Nevertheless, the computed value $F = 5.0 \cdot 10^{-11}$ in comparison with its exact value $F_{\text{exact}} = 6.3 \cdot 10^{-11}$ is fully sufficient for our purposes. For CNTs one can expect even more precise computations, as the geometry is simpler – only one hemisphere is present.

The computational errors come mainly from only two iterations used in the adaptive solver (more iterations would exceed the memory limitation of 256 MB in our computer). Another source of errors originates from boundary condition $\vec{E} \to \vec{E}_0$ for $r \to \infty$, which is from computational reasons approximated by the condition $\vec{E} = \vec{E}_0$ on a large box surrounding the sphere. The reported value $F = 5.0 \cdot 10^{-11}$ has been obtained for the cube box of the length $8R$. For the box of the length $6R$ this result would be somewhat worse, $F = 4.8 \cdot 10^{-11}$.

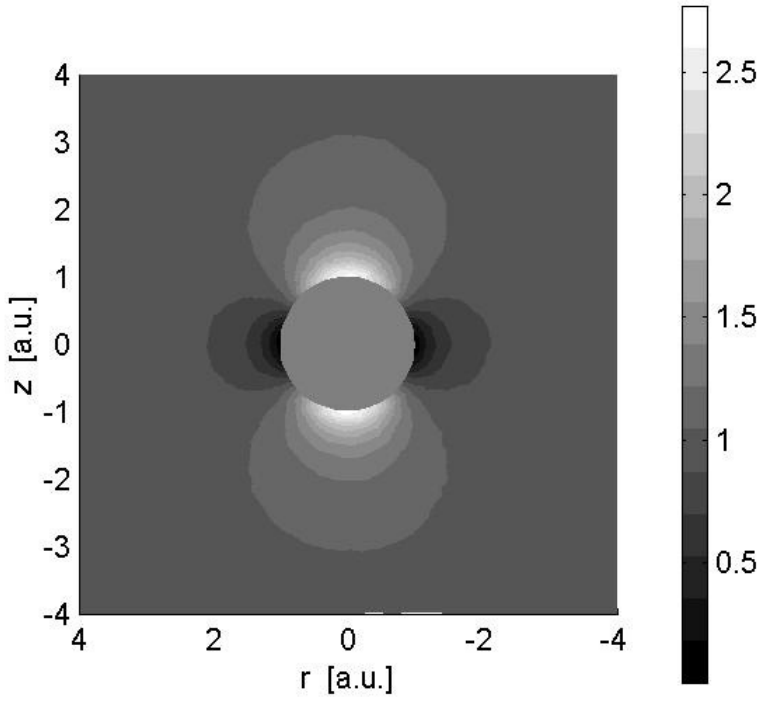

Fig.1 Field enhancement factor $\gamma = E_z / E_0$ for the conductive sphere placed in a homogeneous electrostatic field E_0 oriented vertically (z-direction).

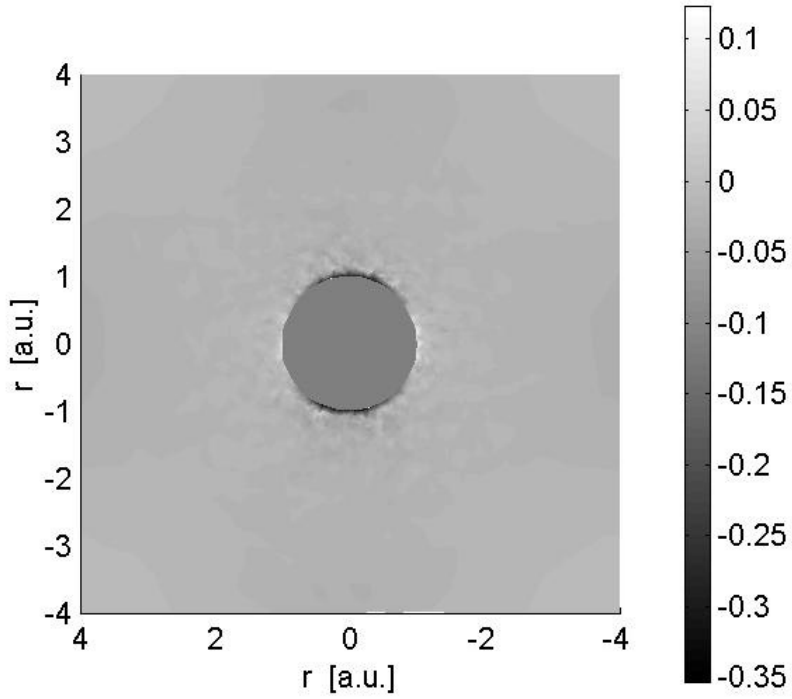

Fig.2 Error γ_{comp} -γ_{exact} for the field from Fig.1 The maximum error of about 30% is reached on the surface of the sphere.

Numeric results for CNTs

Computational investigations in FEMLAB enable broad investigations revealing how the field and force depend on the DC bias, nanotube dimensions, distances between neighboring nanotubes, shapes of their tips and other parameters. The typical numerical value $F \approx 1 \cdot 10^{-14}$ N of the force acting on the nanotube with 20 nm radius is approximately four order of magnitude higher than the weight of the cobalt droplet of the same radius (catalytic particle on the nanotube tip) and is equal to the weight of the amorphous carbon cylinder of the same radius and height of about 350 μm.

Fig.3 depicts the field enhancement factor for the nanotubes with the spherical tips of the radius 20 nm, placed in the distances 70 nm each from other. For the spherical tip the maximum field enhancement factor $\gamma \equiv E/E_0$ is about 2.5. The field between the nanotubes is screened. As the computations showed, the force acting on the nanotube tip depends only weakly on its radius (Fig.4) and shape. On the contrary, this force strongly depends on the distance between two neighboring nanotubes (Fig.5), as more densely placed nanotubes effectively screen the field and the field enhancement factor drops to its "flat" limit 1.

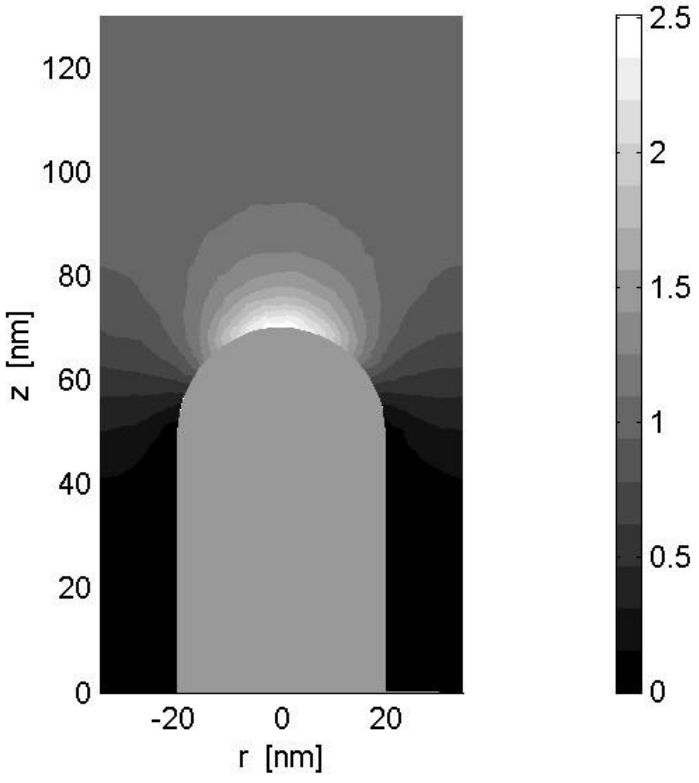

Fig.3 Field enhancement factor $\gamma = E / E_0$ of the electric field close to the nanotube tip of the radius of 20 nm. CNTs are placed at distances 70 nm each from other.

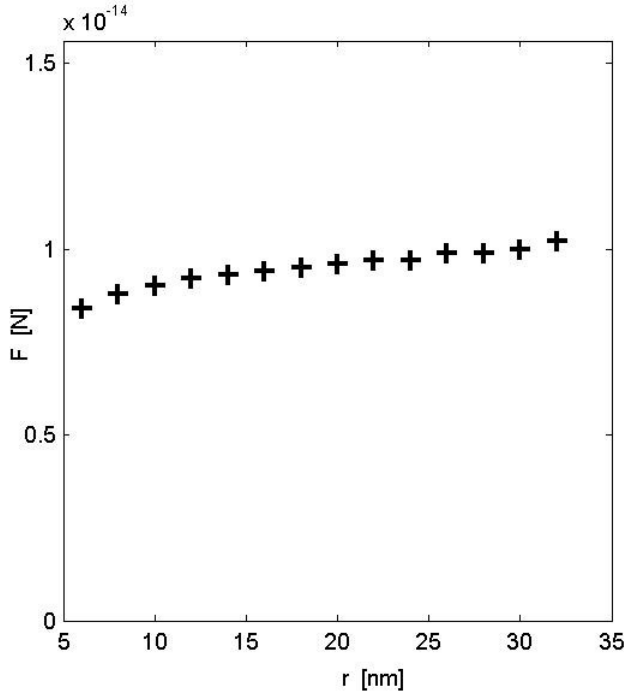

Fig.4 Dependence of the force F on the radius r of the nanotubes. Other parameters including the distance between neighboring nanotubes are kept constant.

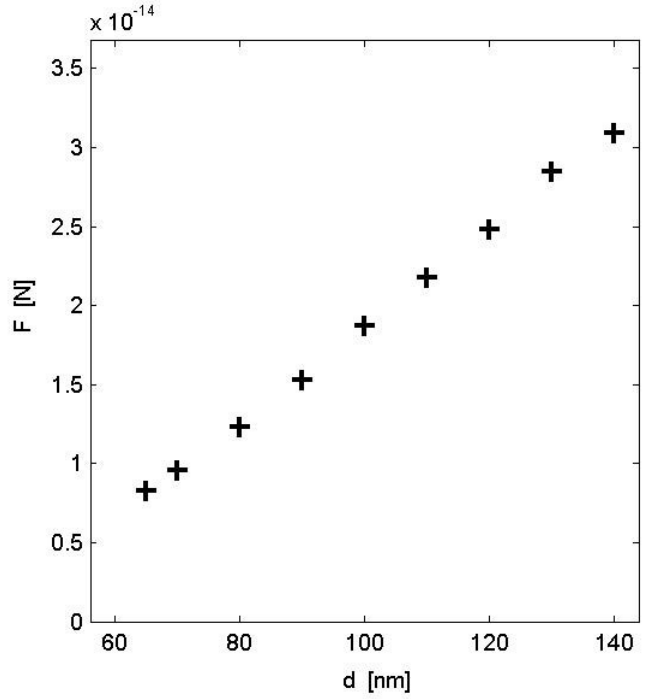

Fig.5 Dependence of electric force F on the distance d between neighboring nanotubes. The other parameters are kept constant.

The experimental data used in our computations as well as the interpretation of numeric results will be published elsewhere [8], but the most important conclusion is as follows: Electric forces acting on carbon nanotubes in a DC plasma sheath with the bias of about 600 V or larger can really bring about - due to their relatively huge values – the CNTs alignment.

Appendix: Electric field of a conductive sphere solved by command-line function

```
% R     radius of the sphere
% d, h  transverse dimensions and height of
%       rectangular box
% E0    homogeneous electric field

% implicit values of R, d, h, E0
if ~exist('R')  R = 1;     end
if ~exist('d')  d = 8*R;   end
if ~exist('h')  h = 8*R;   end
if ~exist('E0') E0 = 1;    end
cc = [R d h E0];
cc = input(['\nparameters R d h E0 (', ...
num2str(cc,'%2g %2g %2g %2g'),') : '],'s');
cc = str2num(cc);
var = {'R','d','h','E0'};
for i = 1:length(cc)
  eval([var{i} ' = cc(i);']);
end
if d < 2*R
  fprintf('It is not d > 2R !\n\n');
  break;
end

% geometry
box = block3(d,d,h,'center');
sph = sphere3(R,[0 0 0],[1 0 0]);
sph = rotate(sph,pi/2,[1 0 0],[0 0 0]);

U = 0;                    % potential of the sphere
eps0 = 8.854e-12;         % permitivity
clear fem;
fem.variables = {'eps0',eps0,'E0',E0,'U',U,'R',R};
fem.geom = box - sph;
fem.mesh = meshinit(fem);

% faces of the box
% lateral:                1 2 5 16
% lower:                  3
% upper:                  4
% faces of the sphere:     6:15
% upper faces:             8 9 11 13 15
% 1st group: V  = -U,  type V
% 2nd group: nD =  0,  type nD0
% 3rd group: nD = -E0, type nD
% face:       1 2 3 4 5 6 7 8 9 10 11 12 13 14 15 16
a.bnd.ind  = [2 2 3 4 2 1 1 1 1  1   1  1  1  1  1  2];
a.bnd.type = { 'V' 'nD0' 'nD' 'nD' };
a.bnd.V    = { '-U' {} {} {} };
a.bnd.nD   = { {} {} 'eps0*E0' '-eps0*E0' };
a.equ.epsilon = 'eps0';
a.equ.rho = 0;

% solution in 3D electrostatics application mode
a.mode = flpdees3d;
fem.appl = {a};
fem = multiphysics(fem);
fem = …
adaption(fem,'Report','on','Stop','on','NGen',2);

% force acting on the upper hemisphere
expr = '-Vz.*ncu/2';
% exact value of the force
Fext = 9/4*pi*eps0*(R*E0)^2;
% computed value of the force
Fcmp = posteint(fem,expr,'Bdl',[8 9 11 13 15]);
fprintf(['\nE0 = %9.2e R = %5.2f  d = %5.2f  ' ...
  'h = %6.2f  'Fcmp = %9.2e  Fext = %9.2e\n\n'], ...
  E0,R,d,h,Fcmp,Fext);

% graphs
% electric field round the sphere
figure;
gamma = posteval(fem,'-Vz/E0','Cont','on');
postplot(fem,'SliceData',gamma,'SliceXSpacing', …
  [0 0],'SliceMap',gray,'SliceBar','on','Cont','on', ...
  'BdL',[6:15],'Tridata','nD','TriMap', …
  [0.5 0.5 0.5],'TriFaceStyle','interp','Axis', …
  [-d/2,d/2,-d/2,d/2 -d/2,d/2],'AxisEqual','on', …
  'View',[-90 0]);
xlabel('r  [a.u.]');
ylabel('r  [a.u.]');
zlabel('z  [a.u.]');
title('\gamma = E_{z}/E_{0}');
% error: gamma(computed) – gamma(exact)
figure;
[z,r] = …
  posteval(fem,'z','sqrt(x.^2+y.^2+z.^2)','Cont','on');
gamma = gamma - 1 - (R./r).^3.*(3*(z./r).^2-1);
postplot(fem,'SliceData',gamma,'SliceXSpacing', …
  [0,0],'SliceMap',gray,'SliceBar','on','BdL',[6:15],…
  'Tridata','nD','TriMap',[0.5 0.5 0.5], …
  'TriFaceStyle','interp', …
  'Axis',[-d/2,d/2,-d/2,d/2 -d/2,d/2], …
  'AxisEqual','on','View',[-90 0]);
xlabel('r  [a.u.]');
ylabel('r  [a.u.]');
```

```
zlabel('z  [a.u.]');
title('Error  \gamma_{comp}- \gamma_{exact}');
% mesh
figure;
expr = ['x > 0 & x < ',num2str(0.7*R)];
meshplot(fem,'EdgeColor','w','BoundMode','off', …
 'ElLogic',expr,'ElLogicType','any');
axis equal off;
view([-50 10]);
title('Finite Element Method - Meshgrid');
% surface charge density induced on the sphere
c = 1.1*R;
figure;
postplot(fem,'TriData','ncu','TriMap',gray, …
 'BdL',[6:15],'Cont','on','TriBar','on', …
 'Axis',[-c,c,-c,c -c,c],'AxisEqual','on','View',[0 0]);
xlabel('x  [a.u.]');
ylabel('y  [a.u.]');
zlabel('z  [a.u.]');
axis off;
title('Surface Charge Density');
% error of computed surface charge density
figure;
expr = 'ncu./(3*eps0*E0)-z/R';
postplot(fem,'TriData',expr,'TriMap',gray, …
 'BdL',[6:15],'Cont','on','TriBar','on', …
 'Axis',[-c,c,-c,c -c,c],'AxisEqual','on','View',[0 0]);
xlabel('x  [a.u.]');
ylabel('y  [a.u.]');
zlabel('z  [a.u.]');
axis off;
title(['Relative Error  (\sigma_{comp}-' …
 '\sigma_{exact}) / \sigma_{max}']);
```


Acknowledgement:

This work was supported by the projects MSM OC527.60, MSM 124100004 and partially DFG LE 863/9-1.

References:

[1] Iijima S.; Nature London 354, 56 (1991)

[2] Ebbesen T.W.; Carbon Nanotubes: Preparation and Properties; Chemical Rupper Corp. Boca Raton, Fl, 1997

[3] Subramoney S.; Adv. Mater. 10, 1157 (1998)

[4] Yu J. et al: Chem. Phys. Letters 232 (2000) 529

[5] Chen Y., Guo L., Patel S., Shaw D.T.: J.Mater.Sci. 35 (2000) 5517

[6] Bower C., Zhu W., Jin S., Zhou O.: Appl.Phys.Letters 77 (2000)

[7] Lieberman M.A., Lichtenberg A.J.: Principles of plasma discharges and materials processing. John Wiley & Sons (1994)

[8] Blažek J., Špatenka P., Pácal F., Täschner Ch., Leonhardt A.; Appl.Phys.Letters (submitted)

Contact:

Josef Blažek
Department of Physics, Faculty of Education
University of South Bohemia
Jeronýmova 10, 371 15 České Budějovice
Czech Republic
E-mail: bla@pf.jcu.cz

Petr Špatenka
Faculty of Biological Sciences
University of South Bohemia
Branišovská 31, 370 05 České Budějovice
Czech Republic
E-mail: spata@tix.bf.jcu.cz